ResearchGate

See discussions, stats, and author profiles for this publication at: https://www.researchgate.net/publication/259930645

On the Challenge of Electrolyte Solutions for Li–Air Batteries: Monitoring Oxygen Reduction and Related Reactions in Polyether Solutions by Spectroscopy and EQCM

DATASET *in* JOURNAL OF PHYSICAL CHEMISTRY LETTERS · DECEMBER 2012

Impact Factor: 7.46 · DOI: 10.1021/jz3017842

CITATIONS
56

READS
102

6 AUTHORS, INCLUDING:

Vinodkumar Etacheri
Purdue University
23 PUBLICATIONS **1,569** CITATIONS
SEE PROFILE

Doron Aurbach
Bar Ilan University
536 PUBLICATIONS **21,869** CITATIONS
SEE PROFILE

Available from: Vinodkumar Etacheri
Retrieved on: 27 January 2016

THE JOURNAL OF PHYSICAL CHEMISTRY Letters

Letter

pubs.acs.org/JPCL

On the Challenge of Electrolyte Solutions for Li–Air Batteries: Monitoring Oxygen Reduction and Related Reactions in Polyether Solutions by Spectroscopy and EQCM

Daniel Sharon,[†] Vinodkumar Etacheri,[†] Arnd Garsuch,[‡] Michal Afri,[†] Aryeh A. Frimer,[†] and Doron Aurbach*,[†]

[†]Department of Chemistry, Bar Ilan University, Ramat-Gan, 52900, Israel

[‡]BASF SE, GCI/E - M311, Ludwigshafen, 67056, Germany

Supporting Information

ABSTRACT: Polyether solvents are considered interesting and important candidates for Li–O_2 battery systems. Discharge of Li–O_2 battery systems forms Li oxides. Their mechanism of formation is complex. The stability of most relevant polar aprotic solvents toward these Li oxides is questionable. Specially high surface area carbon electrodes were developed for the present work. In this study, several spectroscopic tools and in situ measurements using electrochemical quartz crystal microbalance (EQCM) were employed to explore the discharge–charge processes and related side reactions in Li–O_2 battery systems containing electrolyte solutions based on triglyme/lithium bis-(trifluoromethanesulfonyl)imide (LiTFSI) electrolyte solutions. The systematic mechanism of lithium oxides formation was monitored. A combination of Fourier transform infrared (FTIR), NMR, and matrix-assisted laser desorption/ionization (MALDI) measurements in conjunction with electrochemical studies demonstrated the intrinsic instability and incompatibility of polyether solvents for Li–air batteries.

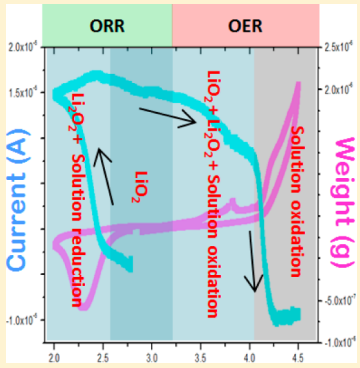

SECTION: Energy Conversion and Storage; Energy and Charge Transport

The great desire to reduce dependency on fossil fuel has pushed researchers to explore novel high energy density rechargeable batteries for electrical propulsion. Lithium–air batteries are particularly attractive because of the huge theoretical energy density (3505 Whkg^{-1}).[1] Although a lot of effort has been put into research over the past decade, the field of nonaqueous Li–air batteries is presently confronted by a number of serious challenges.[2,3] However, perhaps the greatest challenge to the successful introduction of the lithium–air battery is finding compatible and stable electrolyte solutions.[4−7] During the oxygen reduction reaction (ORR), various nucleophilic oxygen species such as O_2^-, O_2^{2-}, and O^{2-} are formed,[8] which attack and mediate oxidation of the electrolyte.[9] The reactions of these lithium oxides and the electrolyte solution degradation have a major effect on the efficiency of Li–air cells by attenuating the cell capacity and the reversibility of the products.[10] In this study we focused on triglyme/lithium bis(trifluoromethanesulfonyl)imide (LiTFSI) as a classical representative of nonvolatile ether-based solutions that may be relevant for Li–air batteries.[11]

In order to investigate the mechanism of the ORR, the formation of lithium oxides species and identification of side reactions, we developed methodology that included the use of high surface area activated carbon fiber electrodes (see images in the Supporting Information (SI)), in order to work at high ratio of electrodes' surface to solution volume, as required for practical battery systems.

These electrodes were measured by scanning electron microscopy (SEM), energy-dispersive X-ray spectroscopy (EDS), X-ray diffraction (XRD), and Fourier transform infrared (FTIR) and the solution phase was measured by NMR and MALDI. We used in situ electrochemical quartz crystal microbalance (EQCM) measurements in conjunction with cyclic voltammetry. For these studies, electrocatalytic Pt on thin quartz crystal electrodes were used.[12] In order to correlate between changes in frequency (Δf) and changes in mass (Δm), in the EQCM measurements, we used the basic Sauerbery equation, which shows a linear relationship between them:[13]

$$\Delta f = -C_m \Delta m$$

where C_m is constant for a specific crystal (more detailed experimental and theoretical EQCM information in the SI). The frequency changes of the quartz crystal (QC) were converted in Figure 1a to changes in the mass of the electrode as a function of potential. The open circuit voltages in the experiments were around 2.7 V (vs Li | Li$^+$), and the potential was scanned between 2 and 4.5 V, at 0.1 mV/s. Scheme 1 presents the main possible redox reactions that can take place during discharge of nonaqueous Li–O_2 cells. The equivalent weights of the products are presented inside the parentheses as

Received: November 4, 2012
Accepted: December 18, 2012
Published: December 18, 2012

ACS Publications © 2012 American Chemical Society

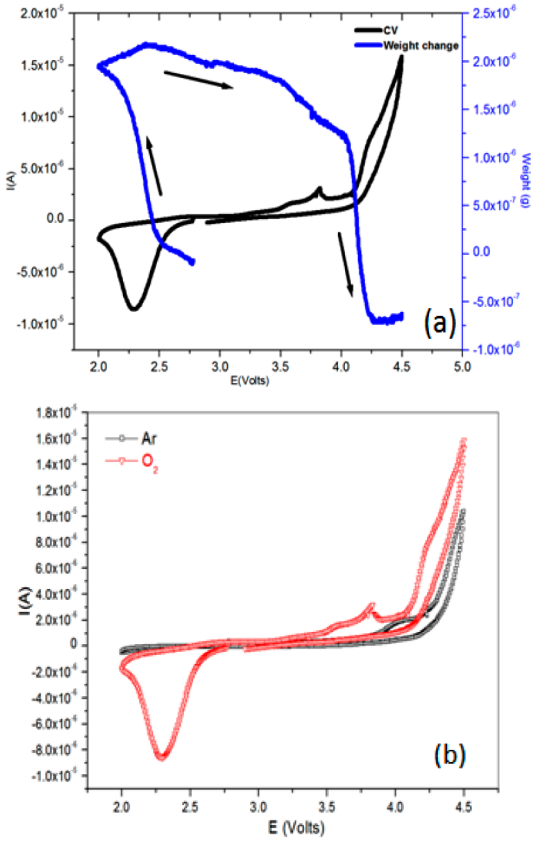

Figure 1. (a) Cyclic voltammetry and EQCM response of ORR (cathodic scan) and OER (anodic scan) in triglyme/LiTFSI 1 M. (b) Cyclic voltammetry of triglyme/LiTFSI 1 M in oxygen and argon atmospheres. WEs were platinum disks deposited on thin quartz crystals.

Scheme 1. Main Redox Reactions Related to O_2 Reduction in Li−O_2 Cells, the Molecular Weight of the Products, and the Expected m.p.e. Values (Mass Accumulated Per Mol of Electrons)

1. $O_2 + Li^+ + e^- \rightleftharpoons LiO_2$ (m.p.e ≈ 39 $g \cdot mol^{-1}$)
2. $2LiO_2 \rightleftharpoons Li_2O_2 + O_2$ (m.p.e ≈ 23 $g \cdot mol^{-1}$)*
3. $LiO_2 + Li^+ + e^- \rightleftharpoons Li_2O_2$ (m.p.e ≈ 7 $g \cdot mol^{-1}$)
4. $2Li^+ + 2e^- + O_2 \rightleftharpoons Li_2O_2$ (m.p.e ≈ 23 $g \cdot mol^{-1}$)
5. $Li_2O_2 + 2e^- + 2Li^+ \rightleftharpoons 2Li_2O$ (m.p.e ≈ 7 $g \cdot mol^{-1}$)

*For a tow electron process that forms 2 LiO_2 that disproportionate to Li_2O_2 and O_2.

shown in Scheme 1.[14] The scheme presents also the relevant mass per moles of electrons (m.p.e.) relevant to the formation and precipitation of the various reactions products.

The first step in the reduction of oxygen in an aprotic electrolyte solution is the formation of the superoxide ion (O_2^-). In the presence of lithium ions, the LiO_2 is generated via reaction 1. This superoxide may be soluble in various organic solutions, which can enhance the operation of Li−air cells by avoiding pore-blockage. Unfortunately, this desirable product is particularly unstable. This results from the crucial influence of the cation on the stability of the superoxide, an observation noted in many studies.[15] The small Li^+ cation forms an unstable lithium superoxide molecule with a very short lifetime that continues to react forming lithium peroxide in either of two ways: by disproportionation (reaction 2); or by electrochemical reduction (reaction 3). [Noteworthy is the fact that because there is no net electron transfer in the disproportionation, it is very difficult to observe this process by only electrochemical methods]. There is also an alternative possibility of a two electron transfer pathway that skips over the formation of LiO_2, and forms Li_2O_2 directly via reaction 4. Proceeding to more negative voltages may result in the reduction of lithium peroxide to lithium oxide (reaction 5).

The EQCM response of oxygen reduction in triglyme//LiTFSI is shown in Figure 1a. The behavior of the mass and current changes in triglyme//LiTFSI shows good fitting between them. This correlates well with the reversibility of lithium oxide formation and dissolution in the polyether electrolyte solution. During the cathodic scan, mass is accumulate on the electrode, and as we sweep the potential back we observe that all the mass is removed from the electrode surface. The slight increase of the mass during the anodic scan at potentials greater than 4.25 (vs Li) probably indicates oxidation of solution species that forms species that accumulate on the electrode (e.g., polymeric species).

The changes in the mass-to-charge ratio, $\Delta m/\Delta Q$, at different regions of potential are listed in Table 1, where all

Table 1. The Mass Per Moles of Electrons (m.p.e.) Response in EQCM during ORR, at Different Potential Domains[a]

ΔE (V)	total weight change (gr)	electron transfer (mol)	m.p.e (g·mol^{-1})
2.7−2.5	2.4×10^{-7}	4.43×10^{-9}	39.28
2.5−2.3	1.57×10^{-6}	2.518×10^{-8}	45.23
2.3−2	8.82×10^{-7}	4.23×10^{-8}	20.94

[a]The three domains were well distinguished according to the different slopes of the mass per charge responses.

of the calculations are for one-electron transfer reactions. The first meaningful piece of data was observed over the range of 2.7−2.5 V, and the calculated molecular weight of the product (39.7 (g mol^{-1})) is very close to that of LiO_2 (38.94 g mol^{-1}). We can, therefore, confirm that the first reaction is the formation of lithium superoxide (Scheme 1, reaction 1). Because of the instability of LiO_2, the next electrochemical step proposed above is the reduction of LiO_2 to Li_2O_2 (Scheme 1, reaction 3). As we lower the potential range to 2.5−2.3 V we detect a mass per electron (m.p.e.) value of 45.2 (g mol^{-1}). For the process $LiO_2 + e^- + Li^+ \rightarrow Li_2O_2$, the expected m.p.e. value should be 7, while for a formation of Li_2O_2 by two electron processes ($O_2 + 2e^- + 2Li^+ \rightarrow Li_2O_2$, or formation of two LiO_2 moieties that disproportionate to $Li_2O_2 + O_2$), the expected m.p.e. should be around 23 g mol^{-1}. The high m.p.e. values calculated for the 2.5−2.3 V domain, indicate that the ORR is complicated by side reactions. We can suggest, as further supported by the spectroscopic studies, that solvent molecules are attacked by the oxides thus formed. Further reduction of LiO_2 species may form highly reactive LiO_2^- moieties that can further attack solvent molecules (especially in the presence of highly electrophilic Li ions around; see scheme 2) to form Li-alkoxide species, which precipitate on the electrode and increase the m.p.e. values. The m.p.e. values calculated for the 2.3−2 V domain, around 21 (g mol^{-1}), seem to correspond well to the formation of Li_2O_2 via two-electron transfer processes (via reaction 4 above). Indeed, we observe accumulation of Li_2O_2 on carbon electrodes as the main

dx.doi.org/10.1021/jz3017842 | J. Phys. Chem. Lett. 2013, 4, 127−131

Scheme 2. Degradation Mechanism of Polyether Solvents during ORR in the Presence of Li Ions

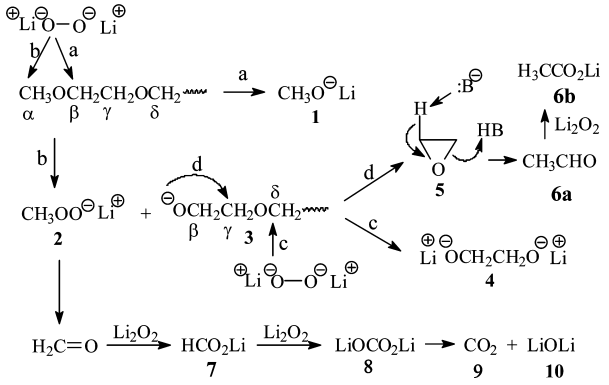

product of oxygen reduction in the presence of Li ions. In a parallel study, we found out that Li_2O_2 in its solid state is not reactive with the triglyme solvent. its seems that highly reactive situation is developed before precipitation of solid Li peroxide, when intermediate oxide anions are formed, so solvent molecules can be attacked by them, with the strong electrophilic assistance of the Li ions in solutions. At low enough potentials (>2.3 V), Li_2O_2 formation and precipitation dominate, and the solid state precipitant thus formed is not too reactive with the solution species. The EQCM data and the relevant calculated m.p.e. values seem to reflect this scenario very well.

We were able to analyze the sequential formation of Li-superoxide and then Li-peroxide and the expected interference of side reactions between the reactive oxides and solutions species.

The same calculations were carried out for the oxygen evolution reaction (OER), which is elaborated in the SI. The main problem with the interpretation of these results is that the OER and the solution oxidation reaction may overlap, at least in the high potential domain of these experiments.[16] As a result, our conclusions for the latter portion of the OER are less clear than those relating to the clear slopes of the EQCM signal in the ORR process. Nevertheless, on the qualitative level, the EQCM response demonstrates a reversible process, as all the mass accumulated on the electrode during the ORR disappears during the OER. In some potential domains such as 3.7−3.9 V, we were able to obtain for the anodic process m.p.e. values close to 23 g mol $^{-1}$ that fit oxidation of Li_2O_2 to O_2 and Li ions (see analysis of the EQCM data in the SI file) .The background CV of triglyme//LiTFSI with argon atmosphere in Figure 1b shows that the electrolyte solution is quite inert during the cathodic sweep. However, throughout the anodic sweep we can observe reactions related to oxidation of the electrolyte solution starting near 4 V. To some extent, the electrochemical window of the electrolyte solution is larger without the presence of oxygen in the system. The EQCM measurements confirm that the ORR forms lithium oxides in the triglyme-based solutions. However, these polyether solvents were expected to be stable to the oxygen radicals, and therefore suitable for Li-air battery systems. Unfortunately, it has been shown in previous studies[17,18]that, even during the very first polarization of the cell, there are pronounced decomposition reactions of the polyether mediated by the reduced oxygen species formed (presumably superoxide and peroxide) in the presence of Li ions. Despite these observations, glymes continue to be used extensively[19] primarily because of their low volatility, good wetting, and reasonable conductivity, as well as their ability to ensure formation of stable lithium oxides at the end of the long discharge process.[11]

To further study the electrolyte solution decomposition during ORR, we constructed cells made from monolithic ACM (activated carbon microfiber) cathodes in triglyme//LiTFSI (1M). The electrochemical performance of these ACM electrodes in triglyme/LiTFSI (1M) are presented in Figure S1 (SI). The SEM images of the pristine electrode in Figure S2 (SI) display cylindrical fibers organized in horizontal and vertical planes to each other. XRD of pristine ACM electrodes, presented in Figure 2a (1), shows only one broad peak at 44°.

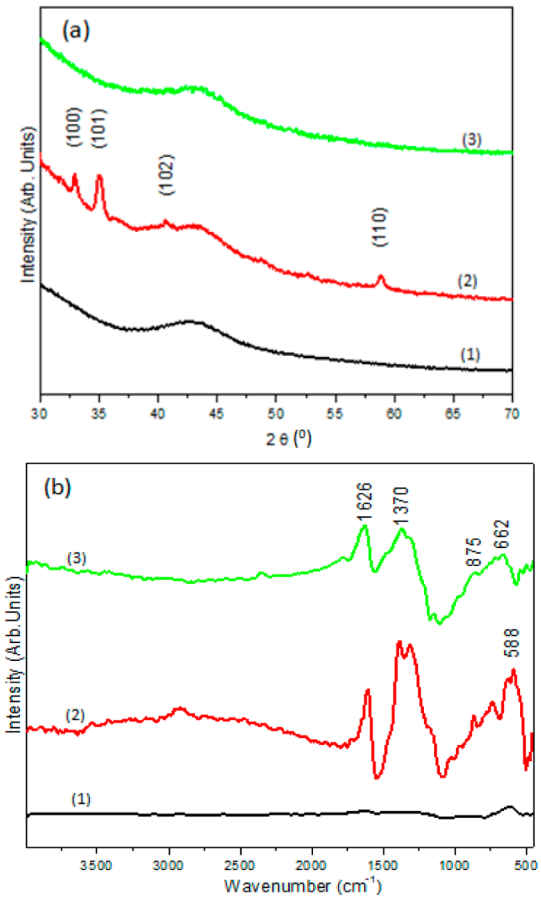

Figure 2. (a) XRD pattern of (1) a pristine ACM electrode, (2) an ACM electrode discharged to 2 V in triglyme/LiTFSI solution, and (3) an ACM electrode that underwent one full cycle, charged to 4.3 V in triglyme/LiTFSI solution. (b) FTIR spectra of (1) a pristine ACM electrode, (2) an ACM electrode discharged once to 2 V in triglyme/LiTFSI solution, and (3) an ACM electrode that underwent a full cycle, charged to 4.3 V in triglyme/LiTFSI solution.

This diffraction corresponds to the (100)/(101) planes of small graphitic structures existing within the amorphous ACM. Figure 2a (2) shows the XRD patterns of the ACM electrode after being discharged to 2.0 V in triglyme/LiTFSI (1 M) under oxygen atmosphere, which exhibit peaks characteristic of crystalline Li_2O_2. The FT-IR spectrum in Figure 2b (2) of the discharged electrode shows a pronounced peak at 588 cm^{-1} that can be assigned to Li_2O_2, Additional FT-IR peaks at 1626, 1370, 875, and 662 cm^{-1} can be attributed to the presence of HCO_2Li, CH_3CO_2Li, and Li_2CO_3. The XRD patterns and the

dx.doi.org/10.1021/jz3017842 | J. Phys. Chem. Lett. 2013, 4, 127−131

FTIR spectra of discharged electrodes, correlate of course with their SEM images (Figure S2), which exhibit uniform coating by toroidal shaped particles that have been identified in previous studies as Li_2O_2 crystals.[20]

The XRD pattern in Figure 2a (3), which belong to a charged electrode (after a full cycle), does not possess any peaks related to Li_2O_2. It is generally similar to that of pristine electrode. The corresponding SEM image of a charged electrode Figure S2 provides us an illustration of the complete decomposition of the toroidal shape Li peroxide particles. The absence of Li_2O_2 in charged electrodes is confirmed from the FTIR spectrum in Figure 2b (3) with the disappearance of the peak located at 588 cm^{-1}. The rest of the FTIR spectrum remained similar to that of the discharged electrode, with irreversible products such as HCO_2Li, CH_3CO_2Li, and Li_2CO_3. These products strongly suggest decomposition of the electrolyte solution during a first cathodic polarization of electrodes in the ethereal solution under oxygen atmosphere.

To fully identify the side products of these reactions, a more comprehensive ORR product analysis for triglyme/LiTFSI was carried out by matrix-assisted laser desorption/ionization (MALDI) mass spectrometry and solution ^1H NMR. Indeed, one of the advantages of using a monolithic ACM cathode is that it enables us to use this MALDI method.[21] The carbon cloth itself could be used as a matrix for the formed products, and no additional matrix was necessary as in ordinary MALDI experiments. The mode of ionization was set for positive voltage, and the resulting fragments are positively charged. Also observed are neutral fragments which are complexed to additional Li^+ or H^+ ions which render the particle positive. In addition, there was no interference from a binder or a catalyst with the ACM electrodes used in the present work.

The m/z values of the major MALDI fragments measured from the discharged electrodes in triglyme/LiTFSI are listed in Figure 3a with the numbering in bold corresponding to compound numbers in mechanistic Scheme 2, discussed later). These fragments were identified as 185 ($[triglyme]Li^+$), 133 ($[CH_3(OCH_2CH_2)_2OLi]Li^+$), 89 ($[CH_3OCH_2CH_2OLi]Li^+$), 81 ($[Li_2CO_3]Li^+$ **8**), 69 ($[CF_3]^+$), 67 ($[CH_3CO_2H]Li^+$, **6b**), 61 ($[CH_3CO_2H]H^+$, **6b**), 55 ($[CH_3OOH]Li^+$, **2**), 45 ($[CH_2CH_2O]H^+$, **5**] and/or $[CH_3CHO]H^+$, **6a**), 39 ($[CH_3OH]Li^+$, **1**), 37 ($[Li_2O]Li^+$, **10**), 33 ($[CH_3OH]H^+$, **1**), 31 ($[Li_2O])H^+$, **10**), and 7 ($[Li^+]$).

Looking at the various fragments, it becomes clear that they can be readily associated with degradation of the electrolyte and to its reaction with lithium peroxide. Before discussing the mechanism of this process, we should comment on the absence of a Li_2O_2 peak. This in fact is not surprising since in a high energy environment Li_2O_2 is known to decompose to Li_2O,[22] which indeed appears in our MALDI spectrum as m/z = 37 [Li_3O^+] and 31 [Li_2OH^+]. The CF_3^+ fragment at m/z = 69 is presumably related to the decomposition of the LiTFSI salt during discharge, and correlates well with the presence of fluorine atoms in the EDS spectrum (Figure S2 Supporting Information).[23,24] In the high mass region, we identify a fragment at 185 which corresponds to a lithium cation chelated by triglyme ($C_8H_{18}O_4Li$). This phenomenon is known from the coupling of lithium cation by 12-crown-4 ($C_8H_{16}O_4Li$).[25]

The NMR spectrum of the triglyme/LiTFSI solution extracted from the cell after one cathodic polarization of the ACM is shown in Figure 3b, and indicates the presence of CH_3CO_2Li (**6b**) and HCO_2Li (**7**).

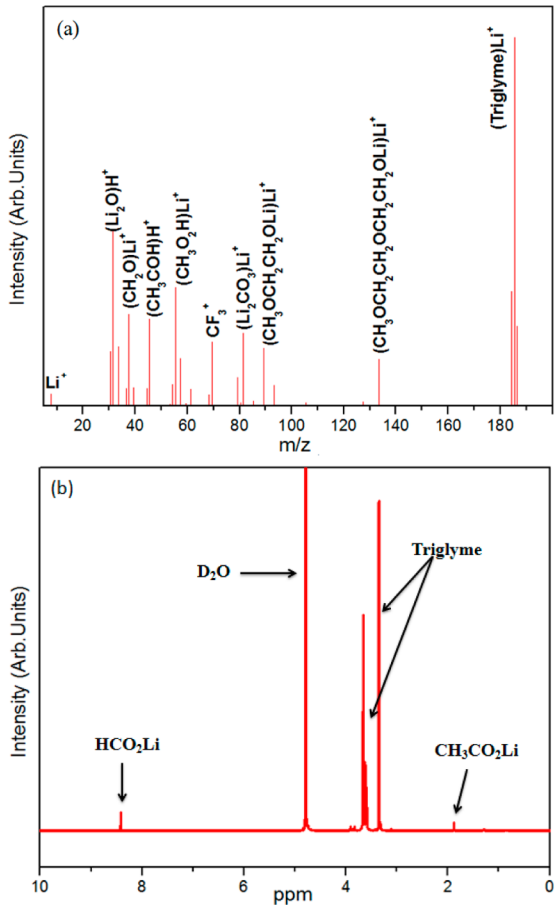

Figure 3. (a) MALDI pattern of an ACM electrode discharged to 2 V in triglyme/LiTFSI solution. (b) ^1H NMR spectra of triglyme/LiTFSI solution taken from the cell after the ACM working electrode was discharged to 2 V (for the first time).

Turning now to the question of mechanism, the formation of the various products can be readily rationalized as resulting primarily from the nucleophilic attack of Li_2O_2 on triglyme, as shown in Scheme 2. We note that the lithium cation is a hard electrophile that is expected to bond strongly to the hard Lewis base oxygen. This in turn helps to convert the alkoxy groups in triglyme into better leaving groups and facilitates nucleophilic attack. Initial attack of Li_2O_2 on the β-carbon of triglyme (path a) generates lithium methoxide (**1**). If attack occurs instead on the terminal α-carbon (path b), methylperoxy lithium (**2**) is formed together with alkoxide **3**. The latter can undergo a second Li_2O_2 attack (path c) generating the dianion of ethylene glycol (**4**). Alternatively, alkoxide **3** can cyclize (path d) yielding oxirane **5**, which rearranges in turn to acetaldehyde (**6a**). This aldehyde, like all other aldehydes in this system, will undergo base-catalyzed autoxidation yielding the corresponding acetic acid (**6b**). Returning to methylperoxy lithium (**2**), base-catalyzed dehydration via the Kornblum−DeLaMare mechanism[26] yields formaldehyde, which undergoes oxidation to lithium formate and dilithium carbonate acid (**7** and **8**).

To conclude, EQCM measurements provided us with a very sensitive in situ method for the detection of lithium oxide formation as a function of potential. The response of the EQCM measurements during ORR in triglyme/LiTFSI solutions reveals a sequential reduction of LiO_2 and Li_2O_2 interfered by reactions of the oxide moieties with solution species. The OER analysis shows that all the products formed

dx.doi.org/10.1021/jz3017842 | J. Phys. Chem. Lett. 2013, 4, 127−131

during the ORR are oxidized and disappear from the electrode. Decomposition of Li_2O_2 (detected separately in a certain voltage domain) is also mixed with side reactions including oxidation of solution species. The products of electrolyte solution degradation have been confirmed by various different methods. However, it would seem that instead of rejecting polyethers as solvents for Li−oxygen battery systems, we perhaps need to investigate the basic chemistry that is causing the solution degradation throughout the ORR. The mechanism that we have presented above can help us find solutions for the protection of ether solvents. Intelligent synthesis of polyether solvents could possibly improve their stability and performance. This can conceivably be done by replacing the hydrogen atoms with more bulky groups or stable atoms, or by combining different additives. The research of screening different electrolytes solutions for these systems should be logical and must consider the potential risks that exist in this chemically active system. A simple trial and error method could substantially delay attaining the goal of developing operative lithium−air batteries.

■ ASSOCIATED CONTENT

Supporting Information

Experimental methods; SEM images, EDS spectra, and electrochemical behavior of carbon electrode. This material is available free of charge via the Internet at http://pubs.acs.org.

■ AUTHOR INFORMATION

Corresponding Author

*E-mail: Doron.Aurbach@biu.ac.il.

Notes

The authors declare no competing financial interest.

■ ACKNOWLEDGMENTS

The research was supported by the BASF scientific network of electrochemistry and batteries.

■ REFERENCES

(1) Xiao, J.; Mei, D.; Li, X.; Xu, W.; Wang, D.; Graff, G. L.; Bennett, W. D.; Nie, Z.; Saraf, L. V.; Aksay, I. a; et al. Hierarchically Porous Graphene as a Lithium−Air Battery Electrode. *Nano Lett.* **2011**, *11*, 5071−5078.

(2) Girishkumar, G.; McCloskey, B.; Luntz, a. C.; Swanson, S.; Wilcke, W. Lithium−Air Battery: Promise and Challenges. *J. Phys. Chem. Lett.* **2010**, *1*, 2193−2203.

(3) Christensen, J.; Albertus, P.; Sanchez-Carrera, R. S.; Lohmann, T.; Kozinsky, B.; Liedtke, R.; Ahmed, J.; Kojic, A. A Critical Review of Li/Air Batteries. *J. Electrochem. Soc.* **2012**, *159*, R1.

(4) Mccloskey, B. D.; Bethune, D. S.; Shelby, R. M.; Girishkumar, G.; Luntz, A. C. Solvents' Critical Role in Nonaqueous Lithium≒Oxygen Battery. *J. Phys. Chem. Lett.* **2011**, 1161−1166.

(5) Garsuch, A.; Badine, D. M.; Leitner, K.; Gasparotto, L. H. S.; Borisenko, N.; Endres, F.; Vracar, M.; Janek, J.; Oesten, R. Investigation of Various Ionic Liquids and Catalyst Materials for Lithium−Oxygen Batteries. *Z. Phys. Chem.* **2012**, *226*, 107−119.

(6) Herranz, J.; Garsuch, A.; Gasteiger, H. A. Using Rotating Ring Disc Electrode Voltammetry to Quantify the Superoxide Radical Stability of Aprotic Li−Air Battery Electrolytes. *J. Phys. Chem. C.* **2012**, *116*, 19084−19094.

(7) Peng, Z.; Freunberger, S. A.; Chen, Y.; Bruce, P. G. A Reversible and Higher-Rate Li−O_2 Battery. *Science (New York, N.Y.)* **2012**, *337*, 563−566.

(8) Peng, Z.; Freunberger, S. A.; Hardwick, L. J.; Chen, Y.; Giordani, V.; Bardé, F.; Novák, P.; Graham, D.; Tarascon, J.-M.; Bruce, P. G. Oxygen Reactions in a Non-aqueous Li^+ Electrolyte. *Angew. Chem., Int. Ed.* **2011**, *50*, 6351−6355.

(9) Aurbach, M. L.; Daroux, P.; Faguy, E.; Yeager, J. D. The Electrochemistry of Noble Metal Electrodes in Aprotic Organic Solvents Containing Lithium Salts. *J. Electroanal. Chem. Interfacial Electrochem.* **1991**, *297*, 225−244.

(10) Xu, W.; Xu, K.; Viswanathan, V. V.; Towne, S. a.; Hardy, J. S.; Xiao, J.; Nie, Z.; Hu, D.; Wang, D.; Zhang, J.-G. Reaction Mechanisms for the Limited Reversibility of Li−O_2 Chemistry in Organic Carbonate Electrolytes. *J. Power Sources* **2011**, *196*, 9631−9639.

(11) Read, J. Ether-Based Electrolytes for the Lithium/Oxygen Organic Electrolyte Battery. *J. Electrochem. Soc.* **2006**, *153*, A96.

(12) Lu, Y.; Gasteiger, H. A.; Shao-horn, Y. Catalytic Activity Trends of Oxygen Reduction Reaction For Nonaqueous Li−Air Batteries. *J. Am. Chem. Soc.* **2011**, *133*, 19048−19051.

(13) Aurbach, D.; Zaban, a. The Application of EQCM to the Study of the Electrochemical Behavior of Propylene Carbonate Solutions. *J. Electroanal. Chem.* **1995**, *393*, 43−53.

(14) Laoire, C. O.; Mukerjee, S.; Abraham, K. M.; Plichta, E. J.; Hendrickson, M. A. Elucidating the Mechanism of Oxygen Reduction for Lithium−Air Battery Applications. *J. Phys. Chem. C* **2009**, *113*, 20127−20134.

(15) Laoire, C. O.; Mukerjee, S.; Abraham, K. M.; Plichta, E. J.; Hendrickson, M. A. Influence of Nonaqueous Solvents on the Electrochemistry of Oxygen in the Rechargeable Lithium−Air Battery. *J. Phys. Chem. C* **2010**, *114*, 9178−9186.

(16) McCloskey, B. D.; Scheffler, R.; Speidel, A.; Bethune, D. S.; Shelby, R. M.; Luntz, a C. On the Efficacy of Electrocatalysis in Nonaqueous Li−O_2 Batteries. *J. Phys. Chem. C* **2011**, *133*, 18038−18041.

(17) Freunberger, S. A.; Chen, Y.; Drewett, N. E.; Hardwick, L. J.; Bardé, F.; Bruce, P. G. The Lithium−Oxygen Battery with Ether-Based Electrolytes. *Angew. Chem., Int. Ed.* **2011**, *50*, 8609−8613.

(18) Younesi, R.; Hahlin, M.; Treskow, M.; Scheers, J.; Johansson, P.; Edstro, K. Ether Based Electrolyte, $LiB(CN)_4$ Salt and Binder Degradation in the Li−O_2 Battery Studied by Hard X-ray Photoelectron Spectroscopy. *J. Phys. Chem. C* **2012**, *116*, 18597−18604.

(19) Jung, H.-G.; Hassoun, J.; Park, J.-B.; Sun, Y.-K.; Scrosati, B. An Improved High-Performance Lithium−Air Battery. *Nat. Chem.* **2012**, *4*, 579−585.

(20) Black, R.; Oh, S. H.; Lee, J.-H.; Yim, T.; Adams, B.; Nazar, L. F. Screening for Superoxide Reactivity in Li−O_2 Batteries: Effect on Li_2O_2/LiOH Crystallization. *J. Am. Chem. Soc.* **2012**, *134*, 2902−2905.

(21) Ren, S.; Zhang, L.; Cheng, Z.; Guo, Y. Immobilized Carbon Nanotubes as Matrix for MALDI-TOF-MS Analysis: Applications to Neutral Small Carbohydrates. *J. Am. Soc. Mass Spectrom.* **2005**, *16*, 333−339.

(22) Ferapontov, Y. A.; Kokoreva, N. V.; Kozlova, N. P.; Ul'yanova, M. A. Thermal Analysis of Lithium Peroxide Prepared by Various Methods. *Russ. J. Gen. Chem.* **2009**, *79*, 891−894.

(23) Etacheri, V.; Geiger, U.; Gofer, Y.; Roberts, G. A.; Stefan, I. C.; Fasching, R.; Aurbach, D. Exceptional Electrochemical Performance of Si-Nanowires in 1,3-Dioxolane Solutions: A Surface Chemical Investigation. *Langmuir* **2012**, *28*, 6175−6184.

(24) Veith, G. M.; Nanda, J.; Delmau, L. H.; Dudney, N. J. Influence of Lithium Salts on the Discharge Chemistry of Li−Air Cells. *J. Phys. Chem. Lett.* **2012**, *3*, 1242−1247.

(25) Pedersen, C. J. Cyclic Polyethers and Their Complexes with Metal Salts. *J. Am. Chem. Soc.* **1967**, *89*, 7017−7036.

(26) Kornblum, N.; DeLaMare, H. E. The Base Catalyzed Decomposition of a Dialkyl Peroxide. *J. Am. Chem. Soc.* **1951**, *73*, 880−881.